Optical stimulation of inferior temporal cortex induces object-specific visual distortions.

Reza Azadi (r.azadi9@gmail.com)
National Institute of Health https://orcid.org/0000-0001-8649-8046
Simon Bohn
National Institute of Health | University of Pennsylvania
Emily Lopez
National Institute of Health
Rosa Lafer-Sousa
National Institute of Health
Karen Wang
National Institute of Health
Mark Eldridge
National Institute of Health
Arash Afraz
NIH https://orcid.org/0000-0002-9979-3674

Research Article

Keywords: perception, vision, optogenetics, inferior temporal cortex, hallucination, area TE, macaque

Posted Date: February 18th, 2022

DOI: https://doi.org/10.21203/rs.3.rs-1331186/v3

Optical stimulation of inferior temporal cortex induces object-specific visual distortions.

Reza Azadi*[1], Simon Bohn*[1,2], Emily Lopez[1], Rosa Lafer-Sousa[1], Karen Wang[1], Mark Eldridge[1], Arash Afraz[1]

* These authors contributed equally to this work.

[1] Laboratory of Neuropsychology, National Institute of Mental Health, NIH, Bethesda, MD 20892, USA

[2] Department of Psychology, University of Pennsylvania, Philadelphia, PA 19104

Abstract:

To be able to effectively restore vision by direct cortical stimulation, we need to understand the perceptual events induced by stimulation of high-level visual cortices. We trained macaque monkeys to detect and report optogenetic impulses delivered to their inferior temporal cortices. In a series of experiments, we observed that detection of cortical stimulation highly depends on the choice of images presented to the eyes and that detection of cortical stimulation is most difficult when the animal fixates on a blank screen. We show that local stimulation of object selective parts of the visual cortex induce perceptual events that are easy to detect as object-dependent distortions of the concurrent contents of vision. These findings invite expanding the scope of visual prosthetics beyond the primary visual cortex.

Keywords: perception, vision, optogenetics, inferior temporal cortex, hallucination, area TE, macaque

Main Text:

Perturbation of neural activity in the visual system alters visual perception (Brindley & Lewin, 1968; Dobelle et al., 1974; Fernández et al., 2021; Foerster, O., 1929; Jonas et al., 2014; Murphey et al., 2009; Parvizi et al., 2012; Rangarajan et al., 2014; Schalk et al., 2017). Understanding the nature of the perceptual events induced by neural perturbations is essential for bridging the causal gap between neuronal activity and vision as a behavior. This knowledge is crucial for identifying the neural underpinnings of visual hallucinations in psychiatric disorders and for developing effective visual prosthetics for patients with severe visual impairment.

Verbal reports of human patients describe two different types of perceptual events induced by stimulation of various parts of the visual system; here we liberally categorize these events as '*hallucination*' and '*distortion*' events (Figure 1.a). Hallucination happens when brain stimulation adds a specific visual element to the contents of perception. For example, stimulation of the primary visual cortex evokes perception of spots of light or dark known as phosphenes (Foerster, O., 1929). Phosphenes are assumed to have an additive nature in that they occur at retinotopically predictable locations in the visual field (Brindley & Lewin, 1968) and their characteristics do not seem to depend on the images cast on the retinae. Similarly, stimulation of face- and color-sensitive subregions of the fusiform gyrus is reported to induce the perception of 'facephenes' (hallucinatory faces) and 'rainbows' respectively, independent of the object being viewed (Jonas et al., 2014; Schalk et al., 2017). Historically, stimulation induced hallucinatory events have provided the main promise and shaped the conceptual framework for the development of visual prosthetics (Fernández et al., 2021). If stimulation of a given cortical location elicits a specific hallucinatory element (eg. a phosphene, facephene, etc.), one can directly merge and mix these hallucinatory elements to restore a rich sense of vision (Bosking et

al., 2017; Dobelle et al., 1974). Nevertheless, stimulation induced 'distortion' events complicate the landscape. In a distortion event cortical stimulation distorts the concurrent contents of visual perception, thus the perceptual outcome of the stimulation depends on both the cortical position as well as the visual input to the brain. For instance, electrical stimulation of human fusiform gyrus is reported to induce 'changes' while the subjects were looking at faces. Subjects described the effects as "Your face metamorphosed." (Parvizi et al., 2012), or "Middle of the eyes twist" (Rangarajan et al., 2014). Notably, while the subject from one of the studies was looking at nonface objects, electrical stimulation with the same parameters elicited less notable perceptual changes (Parvizi et al., 2012). Moreover, stimulations in the face-selective fusiform area can rarely be detected with closed eyes (Murphey et al., 2009), suggesting dependence of the stimulation-induced perceptual event on the visual input. If stimulation of a single position in the cortex induces different perceptual events depending on the state of the rest of the visual system, then the straightforward mix and merge approach for making visual prosthetic devices becomes obsolete, and our understanding of how the visual cortical activity is decoded by the rest of the brain needs to be revised.

While anecdotal human reports provide invaluable insights, high throughput and systematic study of the case is impossible without an appeal to non-human primate research. Phosphenes have been reliably replicated and studied in the primary visual cortex of macaque monkeys (Schiller et al., 2011). Electrical stimulation of macaque middle temporal (MT) cortex, biases the animals' perceptual judgments in direction detection (Salzman et al., 1990), and depth discrimination tasks (DeAngelis et al., 1998). Cortical stimulation of disparity-tuned neurons in area V4 (Shiozaki et al., 2012) and the inferior temporal (IT) cortex (Verhoef et al., 2012) biases depth perception. Stimulation of IT gloss-selective neurons induces corresponding biases in a

gloss discrimination task (Baba et al., 2021). Stimulation of face-selective subregions of IT cortex decreases the threshold for detecting faces (S.-R. Afraz et al., 2006) and optogenetic silencing of small clusters of face-selective neurons takes a toll on the ability to discriminate faces (A. Afraz et al., 2015). Stimulation of face-selective parts of IT cortex is shown to strongly affect match-to-sample performance for faces but not other stimuli (Moeller et al., 2017), a result that is suggestive of face-specific distortions, but can be explained by face hallucinations as well because a hallucinatory face may interact with the match-to-sample task more for faces than the other stimuli. While these studies reveal specific perceptual changes resulting from artificial perturbation of the neural activity, they remain mostly agnostic with respect to the hallucinatory versus distortive nature of those changes.

In this study, we designed a novel psychophysical task to systematically investigate the characteristics of the perceptual events evoked by optogenetic stimulation of the IT cortex in two macaque monkeys (*Macaca mulatta*). Optogenetics offer enticing advantages over electrical stimulation (Roy et al., 2016) but, historically, optogenetic studies often struggle to obtain large behavioral effects in nonhuman primates (Tremblay et al., 2020). The lack of robust behavioral effects may be the result of challenges associated with delivering adequate virus and light to the large primate brain, use of psychophysical tasks biased to prior assumptions, and the constraining nature of acute stimulation preparations. Here we used the Opto-Array (Rajalingham et al., 2021), a novel chronically implantable array of LEDs, to stimulate the same cortical sites across many sessions. We utilized the optogenetic stimulation in the context of a sensitive stimulation-detection task (Dai et al., 2014; May et al., 2014; Murphey & Maunsell, 2007) unrestricted by prior assumptions about function of the stimulated neurons. We trained the animals to behaviorally detect a short optogenetic stimulation impulse delivered to their IT

cortex while fixating at images of various objects and scenes (Figure 1.b). In each trial, following fixation, an image was displayed on the screen for 1 s. In half of the trials, randomly selected, a 200 ms illumination impulse was delivered to IT cortex halfway through the image presentation, and the animal was rewarded for correctly identifying whether the trial did or did not contain cortical stimulation. The image content was independent of whether brain stimulation would or would not occur and the subjects' exclusive behavioral task was to detect if brain stimulation occurred in a given trial. We found this approach produced robust and large behavioral effects. Here we present the results of a series of experiments deploying this tactic, beginning with an experiment designed to determine whether optogenetic stimulation of IT cortex evokes a detectable visual event and culminating with a systematic test of the hallucination versus distortion hypotheses.

An Opto-Array was implanted over the central IT cortex where we had previously injected Adeno Associated Virus 5 (AAV5) expressing excitatory opsin C1V1 under the CaMKII promoter (right and left hemispheres in monkeys Ph and Sp respectively; Figure 1.c). We also implanted an array in the corresponding region of IT in the opposite hemisphere where no virus was injected (control site).

Training Phase Results

The animals learned the task in only a few sessions, yet they were not able to detect cortical illumination over the control sites over the entire course of the training and Experiment 1 (catch trials). Figure 1.d shows the performance of monkey Ph as a function of session number during the training phase (monkey Sp performed similarly). The difference between stimulation report

rate in stimulation and non-stimulation trials became and stayed statistically significant after 4 and 11 sessions, respectively, in monkeys Ph and Sp (Figure 1.d, red and blue lines. arrow: Ph: X^2 (1, N = 1337) = 6.7, p = 0.010 and Sp: 30.4 X^2 (1, N = 1337) = 30.3, p < 0.001). This difference remained significant throughout the training phase (Ph: p < 0.010, Sp: p < 0.001 for each session). In contrast, performance on catch trials (Figure 1.d, yellow line) did not differ from non-stimulation trials (Ph: p > 0.142, Sp: p > 0.054 for each session) implying that on stimulation trials the animal is in fact reporting detection of cortical stimulation, rather than some other artifact of LED illumination, such as heat or light. These results show for the first time that excitatory optogenetic stimulation in IT cortex is behaviorally detectable in monkeys, but are agnostic to the character and nature of the perceptual event.

Experiment 1: the detection profile

To determine if the perceptual event evoked by optogenetic stimulation of IT is visual in nature, monkeys performed the stimulation-detection task with an imageset that consisted of 40 novel images including a condition with no image in which the subject only viewed the uniform gray background (Figure S1.a). In the stimulation trials (50% of trials), we randomly interleaved stimulations of two cortical sites (~3 mm apart). We found that the performance in detection of cortical illumination systematically varies while the animals fixate at different images, creating a unique array of performances for each cortical position that we refer to as the '*detection profile*'. Figure 2.a shows a detection profile for one stimulation site in monkey Ph (see Figure S2 for more). Performance levels were significantly different across the images (permutation test of randomly selected images per trial Ph: p < 0.001, Sp: p < 0.001 for both stimulation sites). The

animals' performance for the 'no image' condition was the lowest in all detection profiles obtained (permutation test of randomly selected images versus no image for each trial Ph: $p <$ 0.001, Sp: $p < 0.001$ for both stimulation sites). These results suggest that the perceptual event evoked by stimulation is visual as its detectability interacts with the visual input.

The detection profiles of the two neighboring stimulated sites in each animal were correlated (Pearson's $r(39) = 0.91$ and 0.82 respectively in Ph and SP; $p < 0.001$ for both subjects) yet significantly different from each other (Figure 2.b for Ph and Figure S3 for Sp). The correlation may result from leakage of light (Rajalingham et al., 2021) and/or shared neural resources as the two sites were only ~3 mm apart. A Pearson's correlation analysis of the hit rates derived from two distinct stimulation sites revealed that the correlation between patterns of performance across the imageset was significantly larger within a stimulation site than across sites (Ph: $p =$ 0.009, Sp: $p = 0.002$). This difference indicates that the detection profile changes with cortical position and doesn't reflect potential image specific variations in attention. Detection profiles were uncorrelated across the two subjects (Pearson's $r(36) > 0.07$ and < 0.29, $p > 0.077$ for all four comparisons).

Experiment 2: stability of the image effects

Experiment 1 reveals that looking at some images helps the animal detect IT stimulation, and that the rank of images for doing so varies across cortical sites and animals. The ability to detect cortical stimulation also likely depends on nonspecific factors such as virus expression heterogeneity and potential tissue build up under the array that may vary the effective cortical illumination power. In Experiment 2 we tested whether the rank order of the images remained

163 constant across different illumination powers (7 different power levels and 5 visual stimuli
164 including the 'no image' condition). Figure 2.c shows the psychometric functions obtained from
165 one stimulation site in Experiment 2 for Monkey Ph (see Figure S4 for more). Illumination had a
166 significant effect on performance (Pearson's correlation: Ph: $r(33) > 0.78$, $p < 0.001$, Sp: $r(53) >$
167 0.79, $p < 0.001$ for both stimulation sites) and the choice of image did so as well (permutation
168 test of randomly selected images per trial Ph: $p < 0.001$, Sp: $p < 0.001$ for both stimulation sites).
169 The no image condition led to the poorest performance in both animals (permutation test of
170 randomly selected images versus no image per trial Ph: $p < 0.001$, Sp: $p < 0.001$ for both
171 stimulation sites).

172 This reveals the robustness of the effect of the visual input in detecting cortical stimulation.
173 While we have aimed to achieve homogeneous expression of the virus across the tissue, as well
174 as the accurate alignment of the array with the cortex, the results of Experiment 2 make it
175 difficult to explain the variation of image rank across cortical positions by the nonspecific factors
176 that may influence effective illumination.

177

178 **Experiment 3: hallucination vs distortion**

179 The results of Experiments 1 and 2 can be explained by variance in the magnitude or quality
180 of perceptual distortions across images. This interpretation implies that stimulation of a given
181 position in IT cortex leads to different distortions for different visual inputs. Alternatively, these
182 results can be explained with the hallucination hypothesis. According to this interpretation,
183 cortical stimulation adds a constant hallucinatory element to the contents of perception, but
184 perceptual detection of this element varies in difficulty due to figure-ground interactions (e.g.

crowding effect) with screen images (Toet & Levi, 1992). However, performance for the "no image" condition remained systematically low in both experiments and all tests. This suggests that subjects actually use the screen images to detect the cortical stimulation, and has important implications which cannot be easily reconciled with the hallucination hypothesis. But the "no image" condition was an unusual condition among multiple visual stimuli and odd-ball psychophysical effects may have contaminated this finding, a shortcoming that inspired Experiment 3.

In order to tease apart these two interpretations, we tested how the attenuation of visibility of screen images affects detection of the cortical event. The animals performed the stimulation-detection task while fixating on randomly presented images of five objects at four visibility levels in addition to a no image condition (Figure S1). Visibility was degraded by reducing the saturation, spatial frequency and contrast of the images. Hypothetically, if the stimulation induces only a hallucinatory percept, decreasing the visibility of the screen image should either not affect detectability of the brain event or should aid detection by decreasing background clutter. On the other hand, if cortical stimulation causes a distortive effect, it would be easier to notice when the screen image is more visible because the perceptual effect would be a function of the visual input (Figure 3.a).

Visibility of the image had a strong effect on stimulation detectability (Figure 3.b and Figure S5; one-way ANOVA Ph: $F(4,16) = 5.24$, $p = 0.006$; Sp: $F(4,16) = 22.33$, $p < 0.001$). Spearman's Ph: $r(20) = 0.71$, $p < 0.001$; Sp: $r(20) = 0.78$, $p < 0.001$). Consistent with the distortion hypothesis, the monkeys' performance increased with the visibility of the visual input; the fully visible stimuli produced significantly higher performance compared with the two lower levels of visibility and with the "no image" condition ($p < 0.001$ and < 0.001 for all comparisons

for monkeys Ph and Sp). These results are consistent with the idea that IT stimulation has a strong distortive effect on perception of visual objects. Although this should be taken carefully as the animals still performed significantly above chance for the uniform gray condition. This might be because of a hallucinatory component that we cannot rule out or the distortion of the screen itself, or both. Further investigations will hopefully push this frontier in the future.

These results reveal that optogenetic stimulation of a ~1 mm^3 (Rajalingham et al., 2021) subregion of IT cortex evokes visual events that are easily detectable by the subject. These events are strongly and selectively enhanced by concurrent object related activity in the visual system and are not psychophysically isolated from the ongoing visual perception as in strong hallucination. Stimulation of a given cortical position with constant physical parameters appears to induce different perceptual distortions depending on the visual input as its detection varies with the choice of the image and depends on the visibility of that image.

The current Opto-Array technology doesn't allow recording of neural activity, limiting the scope of this study to phenomenology of the stimulation-induced events. Yet it is hard not to speculate about the neural underpinnings of the observed effects. Stimulation of ~1 cubic millimeter of tissue (Rajalingham et al., 2021) is expected to engage IT cortex at a scale that still preserves object category selectivity (Lafer-Sousa & Conway, 2013; Sato et al., 2013). The fact that local cortical perturbation of this scale interacts differentially with various objects is consistent with the heterogeneity of object responses across IT cortex. It may be possible to explain the observed perceptual effects by feedforward models that incorporate object selective excitatory/inhibitory inputs to the targeted neurons, thus varying their population sensitivity to the artificial stimulation in the presence of different visual objects. In fact, 'hallucinations' models based on deep convolutional neural networks are very consistent with our findings in that

231 they are structured based on the visual input (Bau et al., 2021; Suzuki et al., 2017). Note that the
232 term hallucination is used in its inclusive definition in these studies. Alternatively, empirical
233 neural recording data may require more complex models that incorporate feedback and cortico-
234 cortical dynamics in order to explain how a complex system responds to local perturbation
235 (Jazayeri & Afraz, 2017). Further modeling and physiology work is required to understand the
236 underlying neural mechanics of a psychophysical landscape that looks promising.

237 These findings invite an investigation of state dependence of phosphenes in primary visual
238 cortex as they might not be as hallucinatory as we have assumed. As for IT neurons, their
239 contribution to perception does not seem to be predetermined by their selectivity profile or
240 category labels and the machinery that reads out IT neural activity seems to interpret it with
241 respect to the global state of the visual system. The distortive nature of the perceptual events
242 observed here alludes to the possibility of using stimulation of IT cortex in visual prosthetics to
243 shape and perceptually organize arrays of phosphenes induced by stimulation of primary visual
244 cortex. All together, we hope this study sparks interest and provides a new approach in the search
245 for a causal framework that explains how the neural state shapes and constrains the phenomenal
246 perceptual state of vision.

Materials and Methods

Surgical procedure

In this study, we performed 3 experiments and collected data from two adult male rhesus monkeys (*Macaca mulatta*), referred to as Sp and Ph. All procedures were conducted in accordance with the guidelines of the National Institute of Mental Health Animal Use and Care Committee.

In a sterile surgery under general anesthesia we performed a craniotomy and opened the dura to access the surface of IT cortex (left hemisphere in Sp, right hemisphere in Ph). We then injected AAV5-CaMKIIa-C1V1(t/t)-EYFP (nominal titer: 8×10^{12} particles/ml) into the cortex. To ensure uniform viral expression and reduce anesthesia-controlled time, we used an injection array(Fredericks et al., 2020) including four 31-gauge needles arranged in a 2×2 mm square. We placed the injection array four times, tiling central IT cortex with sixteen evenly spaced injection sites, resulting in a region of ~ 6mm x 6mm viral expression. Each needle was connected with flexible tubing to a 100 µl Hamilton syringe, and injection was controlled by a microinjection pump (Harvard Apparatus Pump 11 Elite). At each injection site, 10 µl of virus was injected at a 0.5 µl/min rate, for a total volume of injection of 160 uL. Ten minutes were allowed to elapse after each injection before removing the array to allow the virus to diffuse into the cortical tissue.

Several weeks later (12 and 4 weeks in Sp and Ph respectively), in a second surgery, we confirmed the virus expression and implanted an Opto-Array (Blackrock Microsystems) on the injection site. To confirm the viral expression, we used the fluorescent signature of the enhanced yellow fluorescent protein (EYFP) coexpressed with the opsin in transduced cells, by shining a 490-515 nm wavelength light (with a NIGHTSEA Dual Fluorescent Protein Flashlight) and

viewing the cortex through 550 nm longpass filter-goggles (NIGHTSEA). This fluorescent signature was confirmed in Monkey Sp, but not in Monkey Ph. Therefore, in Monkey Ph, before proceeding with the array implantation, we performed a second virus injection similar to the first injection procedure (3 injection array placements, yielding 12 injection sites in a region of 4 x 6 mm; 10 µl of virus injected into each site at 0.5 µl/min rate). Then we implanted an Opto-Array over the injection sites. The Opto-Array was placed directly on the pia mater and sutured to the neighboring dura. Following this, in the same surgery, we implanted a second Opto-Array on a similar area of the IT cortex in the opposite hemisphere (control site: right hemisphere in Sp, and left hemisphere in Ph) where no virus injection was performed.

Apparatus

The experiment was carried out with the monkey head fixed, positioned 57 cm from a 27 in, 3840x2160 pixel, 60 Hz, Dell P2715Qt monitor. Fluorescent room lights were turned on to avoid dark adaptation of the retinae. This was done to minimize the possibility that the monkey would detect the light from the Opto-Array through the skull. To guard against heating cortical tissue by LED activation, temperature on the LED die was monitored by a thermistor inside the Opto-Array at the beginning of each trial and trial delivery was paused if the temperature on the LED die rose more than 3° C above the baseline temperature, and restarted once they were less than 1° C above the baseline. 3° C at the LED die translates to approximately 0.5° C temperature change on the cortical surface; this temperature management regime is detailed in Rajalingham et al. 2021 (Rajalingham et al., 2021). The experiment was controlled with a custom MWorks script (The MWorks Project), running on a Mac Pro 2018. Opto-Arrays were controlled by a Blackrock

LED Driver (Blackrock Microsystems) running a custom firmware version for compatibility with MWorks. Gaze was tracked with an Eyelink 1000 Plus (SR Research). Animals were water-restricted in their cages and received liquid rewards for successfully completing trials.

Behavioral task

Monkeys were trained to perform a detection task in which they were rewarded if they correctly identified whether a trial did or did not contain an optogenetic stimulation impulse. The subject started a trial by fixating on a central fixation point (black-on-white bullseye, 0.4° outer diameter and 0.2° inner diameter) for 500 ms on a gray background. Then, an image (scaled so the largest dimension spanned 8° for most images and 30° for four scenes during training and two scenes in experiment 1) appeared on the screen for 1000 ms while the animal held fixation on a central target. In half of the trials (randomly selected) 500 ms from the image onset, an LED on one of the Opto-Arrays was activated for 200ms. Then the image and central fixation point disappeared and two response targets appeared on the vertical midline (white, 0.4° diameter, 5° above and below center). The subject reported the existence or absence of cortical stimulation by fixating for 100 ms on the corresponding response target to the condition . Then, the response targets disappeared and a unique sound was played for correct and incorrect responses. The subject received a juice reward for a correct response or a punishment of 3.5 s delay for an incorrect response before starting the next trial. Trials with broken fixations or a latency of more than 3 s for choosing a response target were considered as an incorrect response during the experiment and excluded from further analysis. A ~300 ms tone played at the same time the image appeared to indicate that a trial had started.

Throughout the training phase and all the experiments, 50% of the trials were '*no-stimulation.*' The other 50% were trials in which an opto-array was activated. In '*stimulation*' trials (40%-50% of all trials depending on the experiment and monkey, see experimental conditions for details), the opto-array on the virus-expressed site was activated and in '*catch*' trials (0%-10% of all trials) the opto-array on the control site was activated. The catch trials used the same stimulation parameters and were rewarded and punished the same as stimulation trials. Performance above chance level on the catch trials would indicate that the subjects did not truly perform the task by detecting the optogenetic activation of IT neurons. This controlled for the possibility that the subjects might be glimpsing light through the skull, or be detecting a potential perturbation of the neural activities caused by the heat (Owen et al., 2019).

Behavioral Training

Both monkeys were operantly trained on the experimental task using a different set of images than would be used in the subsequent experiments (Figure S1b). To maximize the signal that the monkey was learning to detect, we began training by activating five LEDs simultaneously with power of 10.6 mW and 12.1 mW per LED for Ph and Sp respectively in stimulation trials. To reduce choice bias, we employed a 'correction loop' procedure(Salzman et al., 1992). Under this protocol, if the monkey chose the same incorrect response target more than three times in a row, every subsequently presented trial would be the opposite type until the monkey selected the correct response target. Data collected in correction loops were excluded from analysis. Ph. started the training phase with 2 images and the number of images was gradually increased to 22. Sp. started training with all 22 images, but we eventually reduced the number of images to 1 and

slowly reintroduced the full training set like in Ph. Then, in both monkeys we gradually reduced the number of activated LEDs to one, and illumination power to 4.5 mW in Ph and 9.1 mW in Sp. We introduced catch trials to Ph. after 17 sessions at an initial rate of 5% of all trials, then after 23 sessions increased the rate to 10% of all trials which continued for the rest of training. Catch trials comprising 10% of all trials were included for Sp. in all training sessions. In total, the subjects performed 42 and 48 sessions in the training phase, with 67,115 trials and 41,409 trials respectively for Ph and Sp. Part of the training data is reported in Rajalingham et al., 2021 (Rajalingham et al., 2021).

Experimental conditions and visual stimulus

Experiment 1 contained 40 images and 2 illumination sites for stimulation trials (see Figure S1a for image set and inset in Figure 2b and Figure S3 for schematic of illumination locations) with illumination power of 3.6 mW and 5.4 mW respectively for Ph and Sp. Catch trials were included at a rate of 10% and 2%, and 10 and 13 sessions were performed with a total of 17,033 trials and 16,125 trials, and an overall performance of 84.6% and 84.9% correct (catch trials excluded), respectively for Ph and Sp. Ph only received catch trials to one site on the control array while Sp received catch trials to two sites, randomly interleaved. The performances for detecting cortical stimulation were statistically significant for stimulation trials (Ph: X^2 (1, N = 15320) = 7295.1, $p < 0.001$ and Sp: X^2 (1, N = 15794) = 7714.7, $p < 0.001$) but not for catch trials (Ph: X^2 (1, N = 10370) = 0.02, p = 0.879 and Sp: X^2 (1, N = 8428) = 1.7, p = 0.190).

Experiment 2 contained 5 images, 2 stimulation sites and 7 intensity conditions. The stimulation sites were the same as in experiment 1. The images used in this experiment were a

subset of the images used in experiment 1, with the two highest and two lowest d' image conditions selected (average of the two cortical locations). The fifth image was chosen by calculating which image had the greatest difference in d' between cortical location conditions in experiment 1. Illumination power for "stimulation" trials ranged from 0.4 mW to 5.4 mW for both monkeys and 9 and 12 sessions were performed with 14,941 and 14,056 trials collected with overall performance of 79.6% and 74.7% correct, respectively for Ph and Sp. This experiment included no catch trials.

Experiment 3 contained 5 images and 4 image visibility conditions, plus one "no image" (uniform gray) condition (see Figure S1c for this image set). The "no image" condition occurred as often as any one degraded image condition, creating 21 total conditions. One cortical site was used for this experiment (Site 1 for both monkeys). We selected the top 5 highest d' images from experiment 1 at that cortical site for this imageset and degraded their visibility by reducing their contrast, saturation, and spatial frequency to near gray. To do this, the mean luminance of each image was adjusted to match that of the gray display background. Then, saturation was reduced by multiplying each pixel's chromaticity coordinates (a* and b*, CIELAB 1976) by a scale factor of ⅓, 1/9, and 1/27 for the decreasing visibility levels. Image contrast was reduced by the same operation on the L* dimension (lightness) of the CIELAB color profile, but first the mean L* of the distribution was subtracted from each pixel, then re-added after multiplication by the scale factor, ensuring that the mean luminance of the distribution was unchanged. Finally, the spatial frequency of the Lab-scaled images was reduced by convolving each image with a 2D gaussian smoothing kernel with standard deviations of 0.39, 0.78, and 1.56° for the different visibility level. To ensure that the filtered images blended evenly into the background, padding was added to the edges of the images but care was taken to ensure the presented size was the

same 8° as experiment 1 and 2. Each visibility condition was a combination of one CIELAB scaling factor and one gaussian filter. Illumination power was 3.5 mW and 5.4 mW, and 1 session was performed for each monkey with 2030 and 3193 trials collected with overall performance of 77.8% and 90.9% correct trials, respectively for Ph and Sp.

Data Analysis

Detection performance: we used *d'* as a bias-free measure of performance for detecting cortical stimulation (Green & Swets, 1966) which is estimated by the following equation:

$$d' = Z(H) - Z(F)$$

Where *Z* is Z-transform, *H* is the animal's hit rate for detecting stimulation, and *F* is the false alarm rate representing the proportion of trials where no stimulation was applied but the animals reported the trial as stimulated.

Effect of image on detectability (Experiment 1): first, we calculated a *d'* for each image, indicating the detectability of cortical stimulation. This creates a 'detection profile' shown in Figure 2.a and Figure S1. The 95% confidence intervals are estimated for each image by bootstrapping the data, resampling 10,000 times with replacement (Efron, 1992) and the violin plots represent the distribution of the bootstrapped data. To statistically test the effect of image on detectability of cortical stimulation, we ran a permutation test in which first we calculated the standard deviation of the *d'*s across images (observed standard deviation). Then, we generated the null distribution by randomly assigning the images to the trials with 10,000 replications and compared the observed standard deviation to the distribution of standard deviations generated

401 from the null model. The permutation tests showed that the effect of images on detection of
402 cortical stimulation is statistically significant ($p < 0.001$ for all the detection profiles). Moreover,
403 we ran the same permutation tests after excluding the no image trials from the data and the result
404 remained statistically significant ($p < 0.001$ for all the detection profiles).

405 **Effect of cortical stimulation location on image detection profile (Experiment 1):** we
406 used Pearson's correlation to evaluate the similarity between the detection profiles derived from
407 two neighboring stimulation sites. First we calculated a hit rate for each image and each
408 stimulation site. The correlations between hit rate profiles at neighboring sites were statistically
409 significant (Pearson's $r(39) = 0.91$ and 0.82 respectively in Ph and SP; $p < 0.001$ for both
410 subjects). To determine if there was a difference between the sites, we followed up these results
411 with bootstrapped estimates of the correlations within each site and between them, resampled
412 10,000 times with replacement. The median correlation coefficients were 0.95 and 0.95 within
413 the sites, and 0.86 between the sites for Ph (Figure 2.b) and 0.89 and 0.95 within and 0.75
414 between for Sp (Figure S3). These results show that the detection profiles are more correlated
415 within the sites compared with between sites in both subjects. To test if this is a statistically
416 significant difference, we generated a null distribution by randomly assigning sites to the
417 stimulation trials with 10,000 replications; the results of this permutation test show that the
418 observed correlation between the sites is smaller than the correlation between sites in the null
419 distribution derived by randomly assigning sites to the trials (Ph: $p =< 0.010$, Sp: $p < 0.001$;
420 Figure 2.b and Figure S3).

421 **Effect of illumination power on image detection profile (Experiment 2):** in Figure 2.c and
422 Figure S4, we plotted *d'*s as a function of illumination power for each image. We used the
423 following formula to fit the data:

$$d_i' = \alpha x_i^{\beta+\beta_1\lambda_i^1+\beta_2\lambda_i^2+\ldots+\beta_5\lambda_i^5}$$

Where i is the trial number. x is illumination power, α, β, β_1, …, β_n are the fit coefficients. For each trial, the λ that matches the image index is assigned 1, and the rest are assigned 0. Therefore, β_1, β_2, …, β_5 represent the effect of the image on the psychometric functions. The range of r^2s are from 0.89 to 0.98 and 0.83 to 0.95 with the average of 0.94 and 0.89 for both stimulation sites respectively for Ph and Sp. Then we calculated the standard deviation of the coefficients β_1, β_2, …, β_5. A permutation test was performed by assigning random image indices to the trials (10,000 times repetitions) to generate the null distribution of standard deviation for these coefficients. The results showed a significant effect of images on psychometric functions ($p < 0.001$ for both sites on both subjects).

References

Afraz, A., Boyden, E. S., & DiCarlo, J. J. (2015). Optogenetic and pharmacological suppression of spatial clusters of face neurons reveal their causal role in face gender discrimination. *Proceedings of the National Academy of Sciences of the United States of America*, *112*(21), 6730–6735. https://doi.org/10.1073/pnas.1423328112

Afraz, S.-R., Kiani, R., & Esteky, H. (2006). Microstimulation of inferotemporal cortex influences face categorization. *Nature*, *442*(7103), 692–695. https://doi.org/10.1038/nature04982

Baba, M., Nishio, A., & Komatsu, H. (2021). Relationship Between the Activities of Gloss-Selective Neurons in the Macaque Inferior Temporal Cortex and the Gloss Discrimination Behavior of the Monkey. *Cerebral Cortex Communications*, *2*(1), tgab011. https://doi.org/10.1093/texcom/tgab011

Bau, D., Andonian, A., Cui, A., Park, Y., Jahanian, A., Oliva, A., & Torralba, A. (2021). Paint by Word. In *arXiv [cs.CV]*. arXiv. http://arxiv.org/abs/2103.10951

Bosking, W. H., Beauchamp, M. S., & Yoshor, D. (2017). Electrical Stimulation of Visual Cortex: Relevance for the Development of Visual Cortical Prosthetics. *Annual Review of Vision Science*, *3*, 141–166. https://doi.org/10.1146/annurev-vision-111815-114525

Brindley, G. S., & Lewin, W. S. (1968). The sensations produced by electrical stimulation of the visual cortex. *The Journal of Physiology*, *196*(2), 479–493. https://doi.org/10.1113/jphysiol.1968.sp008519

Dai, J., Brooks, D. I., & Sheinberg, D. L. (2014). Optogenetic and electrical microstimulation systematically bias visuospatial choice in primates. *Current Biology: CB*, *24*(1), 63–69. https://doi.org/10.1016/j.cub.2013.11.011

DeAngelis, G. C., Cumming, B. G., & Newsome, W. T. (1998). Cortical area MT and the perception of stereoscopic depth. In *Nature* (Vol. 394, Issue 6694, pp. 677–680). https://doi.org/10.1038/29299

Dobelle, W. H., Mladejovsky, M. G., & Girvin, J. P. (1974). Artifical vision for the blind: electrical stimulation of visual cortex offers hope for a functional prosthesis. *Science*, *183*(4123), 440–444. https://doi.org/10.1126/science.183.4123.440

Efron, B. (1992). Bootstrap Methods: Another Look at the Jackknife. In S. Kotz & N. L. Johnson (Eds.), *Breakthroughs in Statistics: Methodology and Distribution* (pp. 569–593). Springer New York. https://doi.org/10.1007/978-1-4612-4380-9_41

Fernández, E., Alfaro, A., Soto-Sánchez, C., Gonzalez-Lopez, P., Lozano, A. M., Peña, S., Grima, M. D., Rodil, A., Gómez, B., Chen, X., Roelfsema, P. R., Rolston, J. D., Davis, T. S., & Normann, R. A. (2021). Visual percepts evoked with an intracortical 96-channel microelectrode array inserted in human occipital cortex. *The Journal of Clinical Investigation*, *131*(23). https://doi.org/10.1172/JCI151331

Foerster, O. (1929). Beitrage zur pathophysiologie der sehbahn und der sehsphare. *J. Psychol. Neurol., Lpz.*, *39*, 463. https://ci.nii.ac.jp/naid/10027785121/

Fredericks, J. M., Dash, K. E., Jaskot, E. M., Bennett, T. W., Lerchner, W., Dold, G., Ide, D., Cummins, A. C., Der Minassian, V. H., Turchi, J. N., Richmond, B. J., & Eldridge, M. A. G. (2020). Methods for mechanical delivery of viral vectors into rhesus monkey brain. *Journal of Neuroscience Methods*, *339*, 108730. https://doi.org/10.1016/j.jneumeth.2020.108730

Green, D. M., & Swets, J. A. (1966). *Signal detection theory and psychophysics* (Vol. 1). Wiley New York.

Jazayeri, M., & Afraz, A. (2017). Navigating the Neural Space in Search of the Neural Code. *Neuron*, *93*(5), 1003–1014. https://doi.org/10.1016/j.neuron.2017.02.019

Jonas, J., Maillard, L., Frismand, S., Colnat-Coulbois, S., Vespignani, H., Rossion, B., & Vignal, J.-P. (2014). Self-face hallucination evoked by electrical stimulation of the human brain. *Neurology*, *83*(4), 336–338. https://doi.org/10.1212/WNL.0000000000000628

Lafer-Sousa, R., & Conway, B. R. (2013). Parallel, multi-stage processing of colors, faces and shapes in macaque inferior temporal cortex. *Nature Neuroscience*, *16*(12), 1870–1878. https://doi.org/10.1038/nn.3555

May, T., Ozden, I., Brush, B., Borton, D., Wagner, F., Agha, N., Sheinberg, D. L., & Nurmikko, A. V. (2014). Detection of optogenetic stimulation in somatosensory cortex by non-human primates--towards artificial tactile sensation. *PloS One*, *9*(12), e114529. https://doi.org/10.1371/journal.pone.0114529

Moeller, S., Crapse, T., Chang, L., & Tsao, D. Y. (2017). The effect of face patch microstimulation on perception of faces and objects. *Nature Neuroscience*, *20*(5), 743–752. https://doi.org/10.1038/nn.4527

Murphey, D. K., & Maunsell, J. H. R. (2007). Behavioral detection of electrical microstimulation in different cortical visual areas. *Current Biology: CB*, *17*(10), 862–867. https://doi.org/10.1016/j.cub.2007.03.066

Murphey, D. K., Maunsell, J. H. R., Beauchamp, M. S., & Yoshor, D. (2009). Perceiving electrical stimulation of identified human visual areas. *Proceedings of the National Academy of Sciences of the United States of America*, *106*(13), 5389–5393. https://doi.org/10.1073/pnas.0804998106

Owen, S. F., Liu, M. H., & Kreitzer, A. C. (2019). Thermal constraints on in vivo optogenetic

manipulations. *Nature Neuroscience*, *22*(7), 1061–1065. https://doi.org/10.1038/s41593-019-0422-3

Parvizi, J., Jacques, C., Foster, B. L., Witthoft, N., Rangarajan, V., Weiner, K. S., & Grill-Spector, K. (2012). Electrical stimulation of human fusiform face-selective regions distorts face perception. *The Journal of Neuroscience: The Official Journal of the Society for Neuroscience*, *32*(43), 14915–14920. https://doi.org/10.1523/JNEUROSCI.2609-12.2012

Rajalingham, R., Sorenson, M., Azadi, R., Bohn, S., DiCarlo, J. J., & Afraz, A. (2021). Chronically implantable LED arrays for behavioral optogenetics in primates. *Nature Methods*, *18*(9), 1112–1116. https://doi.org/10.1038/s41592-021-01238-9

Rangarajan, V., Hermes, D., Foster, B. L., Weiner, K. S., Jacques, C., Grill-Spector, K., & Parvizi, J. (2014). Electrical stimulation of the left and right human fusiform gyrus causes different effects in conscious face perception. *The Journal of Neuroscience: The Official Journal of the Society for Neuroscience*, *34*(38), 12828–12836. https://doi.org/10.1523/JNEUROSCI.0527-14.2014

Roy, A., Osik, J. J., Ritter, N. J., Wang, S., Shaw, J. T., Fiser, J., & Van Hooser, S. D. (2016). Optogenetic spatial and temporal control of cortical circuits on a columnar scale. *Journal of Neurophysiology*, *115*(2), 1043–1062. https://doi.org/10.1152/jn.00960.2015

Salzman, C. D., Britten, K. H., & Newsome, W. T. (1990). Cortical microstimulation influences perceptual judgements of motion direction. *Nature*, *346*(6280), 174–177. https://doi.org/10.1038/346174a0

Salzman, C. D., Murasugi, C. M., Britten, K. H., & Newsome, W. T. (1992). Microstimulation in visual area MT: effects on direction discrimination performance. *The Journal of Neuroscience: The Official Journal of the Society for Neuroscience*, *12*(6), 2331–2355.

https://www.ncbi.nlm.nih.gov/pubmed/1607944

Sato, T., Uchida, G., Lescroart, M. D., Kitazono, J., Okada, M., & Tanifuji, M. (2013). Object representation in inferior temporal cortex is organized hierarchically in a mosaic-like structure. *The Journal of Neuroscience: The Official Journal of the Society for Neuroscience*, *33*(42), 16642–16656. https://doi.org/10.1523/JNEUROSCI.5557-12.2013

Schalk, G., Kapeller, C., Guger, C., Ogawa, H., Hiroshima, S., Lafer-Sousa, R., Saygin, Z. M., Kamada, K., & Kanwisher, N. (2017). Facephenes and rainbows: Causal evidence for functional and anatomical specificity of face and color processing in the human brain. *Proceedings of the National Academy of Sciences of the United States of America*, *114*(46), 12285–12290. https://doi.org/10.1073/pnas.1713447114

Schiller, P. H., Slocum, W. M., Kwak, M. C., Kendall, G. L., & Tehovnik, E. J. (2011). New methods devised specify the size and color of the spots monkeys see when striate cortex (area V1) is electrically stimulated. *Proceedings of the National Academy of Sciences of the United States of America*, *108*(43), 17809–17814. https://doi.org/10.1073/pnas.1108337108

Shiozaki, H. M., Tanabe, S., Doi, T., & Fujita, I. (2012). Neural activity in cortical area V4 underlies fine disparity discrimination. *The Journal of Neuroscience: The Official Journal of the Society for Neuroscience*, *32*(11), 3830–3841. https://doi.org/10.1523/JNEUROSCI.5083-11.2012

Suzuki, K., Roseboom, W., Schwartzman, D. J., & Seth, A. K. (2017). A Deep-Dream Virtual Reality Platform for Studying Altered Perceptual Phenomenology. *Scientific Reports*, *7*(1), 15982. https://doi.org/10.1038/s41598-017-16316-2

Toet, A., & Levi, D. M. (1992). The two-dimensional shape of spatial interaction zones in the parafovea. *Vision Research*, *32*(7), 1349–1357. https://doi.org/10.1016/0042-

6989(92)90227-a

Tremblay, S., Acker, L., Afraz, A., Albaugh, D. L., Amita, H., Andrei, A. R., Angelucci, A., Aschner, A., Balan, P. F., Basso, M. A., Benvenuti, G., Bohlen, M. O., Caiola, M. J., Calcedo, R., Cavanaugh, J., Chen, Y., Chen, S., Chernov, M. M., Clark, A. M., … Platt, M. L. (2020). An Open Resource for Non-human Primate Optogenetics. *Neuron*, *108*(6), 1075–1090.e6. https://doi.org/10.1016/j.neuron.2020.09.027

Verhoef, B.-E., Vogels, R., & Janssen, P. (2012). Inferotemporal cortex subserves three-dimensional structure categorization. *Neuron*, *73*(1), 171–182. https://doi.org/10.1016/j.neuron.2011.10.031

Acknowledgements:

We thank Nanami Miyazaki, and Emilia Jaskot for their critical help in the injection surgeries; Elia Shahbazi and Timothy Ma for their help with designing the implants; and Chris Stawarz and Andrew Mitz for their help with Opto-Array setup.

Funding:

This research was supported by the Intramural Research Program of the NIMH ZIAMH002958 (to A.A.).

Author contributions:

S.B., R.A., E.L. and R.L. designed research with guidance from A.A; S.B., E.L., R.A., R.L., K.W. and M.E. performed research; R.A., S.B. and E.L. analyzed data; R.A., S.B. and R.L. prepared figures; R.A., S.B., R.L., and A.A. wrote the manuscript; all authors reviewed the manuscript.

Competing interests:

The authors declare that there is no conflict of interest.

Data and material availability:

The data and material that support the findings of this study are available on request from the corresponding author R.A.

Figures:

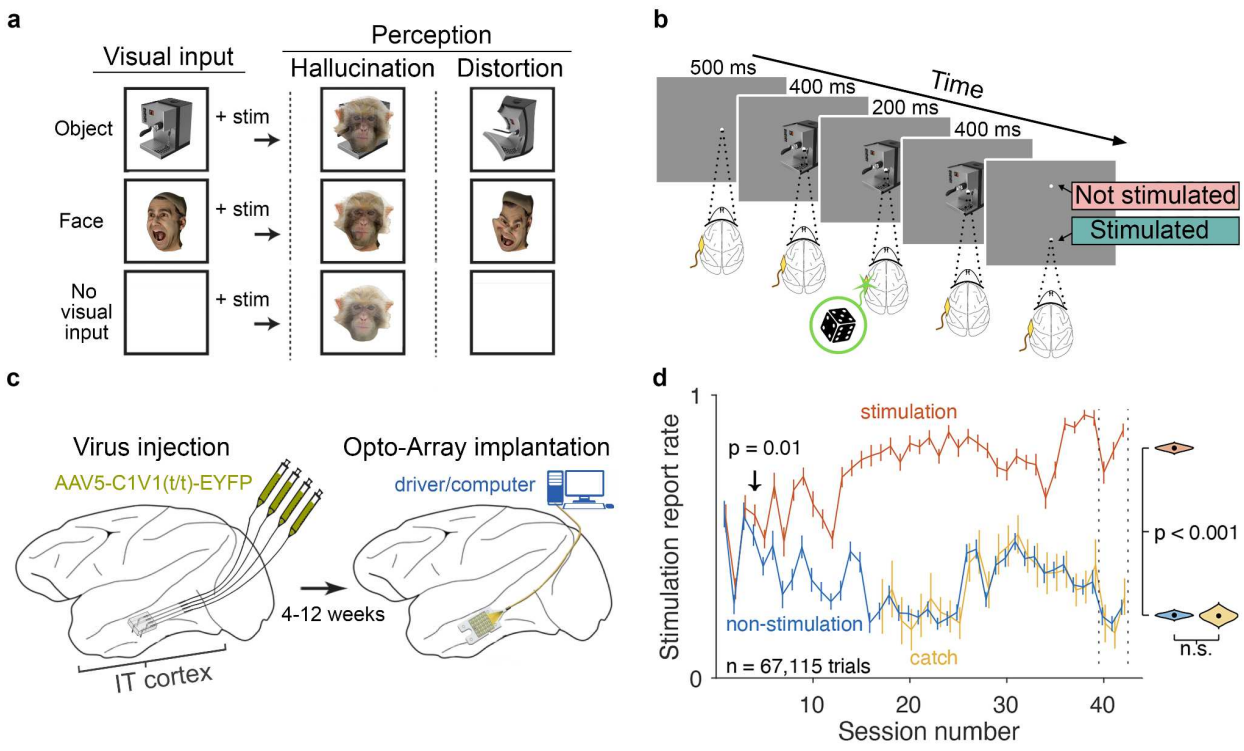

Figure 1. Hypothesis, behavioral task, surgical procedure and training phase results. **a)** Schematic illustration of two hypothetical perceptual events evoked by cortical stimulation. The left column illustrates three different examples of visual stimuli presented on the screen during cortical stimulation. The middle and the right columns demonstrate the two hypotheses: The hallucination hypothesis (middle column) implies that cortical stimulation adds a specific visual element (e.g. a monkey face) to the contents of visual perception independent of the external visual stimulus. Alternatively, the distortion hypothesis (right column) assumes that stimulation-induced perceptual events highly depend on the visual input, predicting a unique event for each visual stimulus viewed. **b)** Behavioral task: in each behavioral trial following fixation an image was displayed on the screen for 1 s. In half of the trials, randomly selected, a 200 ms illumination impulse was delivered to IT cortex halfway through image presentation. The animal was rewarded for correctly identifying whether the trial did or did not contain cortical stimulation by looking at one of the two subsequently presented targets at the end of trial. **c)** Schematic illustration of the procedure for chronic optogenetic stimulation of IT cortex. Left, Injection of

AAV5 expressing the excitatory opsin C1V1. Right, Opto-Array implantation: in a separate surgery, we visually confirmed the expression of the excitatory virus and implanted an Opto-Array over the expression zone. We implanted a second array in the corresponding region of the opposite hemisphere where no virus was injected (control site, not shown). **d)** Behavioral performance of monkey Ph as a function of session number during the training phase. The y-axis indicates the proportion of the trials reported as stimulated. Red, blue and yellow colors represent data from the stimulation, non-stimulation, and catch trials respectively. Error bars represent bootstrapped 95% confidence intervals. The difference between stimulated and nonstimulated trials became significant at session 4 (arrow) and remained so through the training. Fluctuations of performance in time represent usage of different visual stimuli and stimulation intensities throughout the training. No significant difference was found between the catch and non-stimulation trials. The violin plots on the right side illustrate the mean and bootstrapped 95% confidence interval of stimulation report rate for each trial type in the last 3 sessions, between the dashed lines.

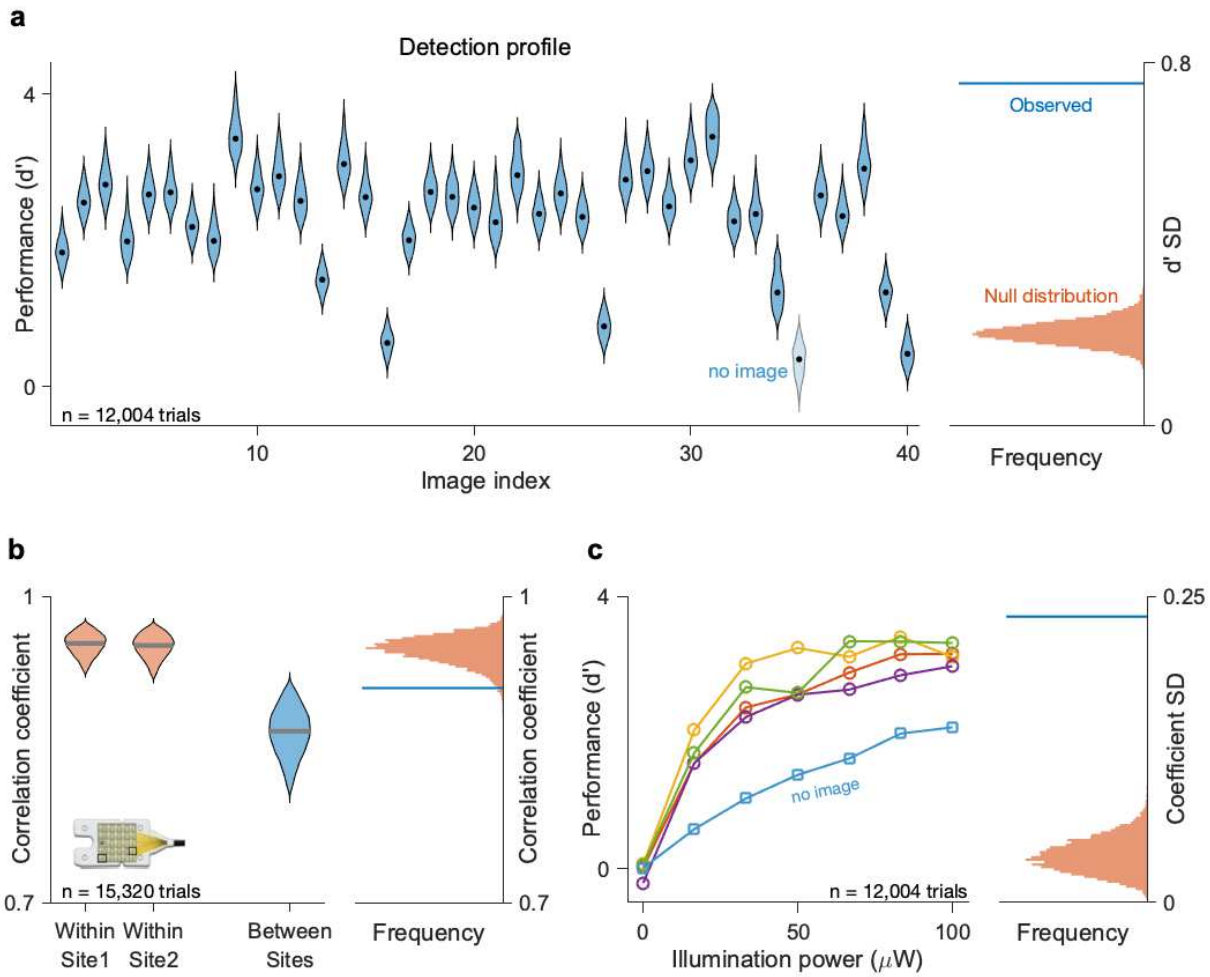

607

608 **Figure 2.** Stimulation detection performance is modulated by visual input, cortical location,
609 and illumination power. **a)** left, detection profile: the behavioral performance (d') on the cortical
610 stimulation detection task for 40 images. The black dots represent d' for each image and the
611 violin plots represent bootstrapped 95% confidence intervals. Right, permutation test: the blue
612 line indicates the standard deviation of d's across images, and the red histogram represents
613 results from a permutation test with 10,000 times randomly assigned images on trials revealing
614 the statistical significance of the effect of image on performance. **b)** left, correlation between
615 detection profiles within each cortical stimulation site and between them. The violin plots
616 represent 95% confidence intervals of the bootstrapped distribution of the correlations with
617 10,000 resamples, and the horizontal lines indicate their medians. Right, permutation test: the
618 blue line indicates the observed correlation between the sites. The red histogram represents
619 results from a permutation test with 10,000 times random assignment of stimulation condition

over the trials. This shows that the correlation of detection profile patterns between the sites is significantly lower than the null distribution. **c)** left, detection performance (d'), as a function of illumination power. Each line represents data from 1 image (5 images in total including the no image condition). Right, permutation test, the standard deviation of the coefficients for each image, derived from fitting of the psychometric curves. The blue line indicates the observed value, and the red distribution represents the null distribution generated by 10,000 times randomly assigning the image indexes to the trials. This confirms the coefficients are significantly different from each other.

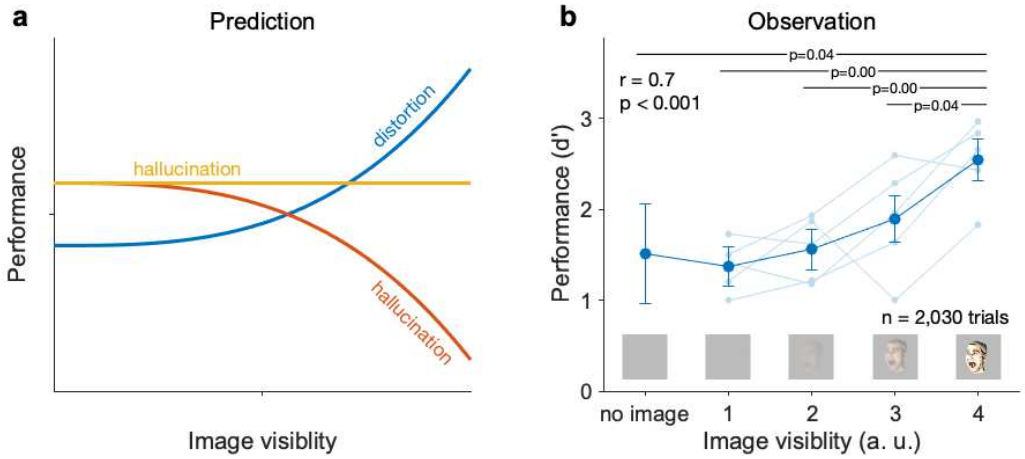

628

629 **Figure 3.** Stimulation detection performance is modulated by image visibility. **a)** prediction:
630 in case of hallucination, decreasing the visibility of the screen image should either not affect
631 detectability of cortical stimulation (yellow line) or help it by decreasing background clutter (red
632 line). In case of distortion, increasing the visibility should increase the detection performance
633 (blue line), since the perceptual effect is a function of the visual input. **b)** observation: the x-axis
634 represents 4 levels of image visibility and the gray background, used in experiment 3. The y-axis
635 is the detection performance (d') on the cortical stimulation detection task. The thin lines
636 represent data from 5 different images and the thick line illustrates the overall averages. Error
637 bars represent 95% confidence intervals. There is a significant correlation between the image
638 visibility and performance (r = 0.7). The p-values for pairwise comparisons are from post-hoc
639 tests of ANOVA (Benjamini-Hochberg corrected).

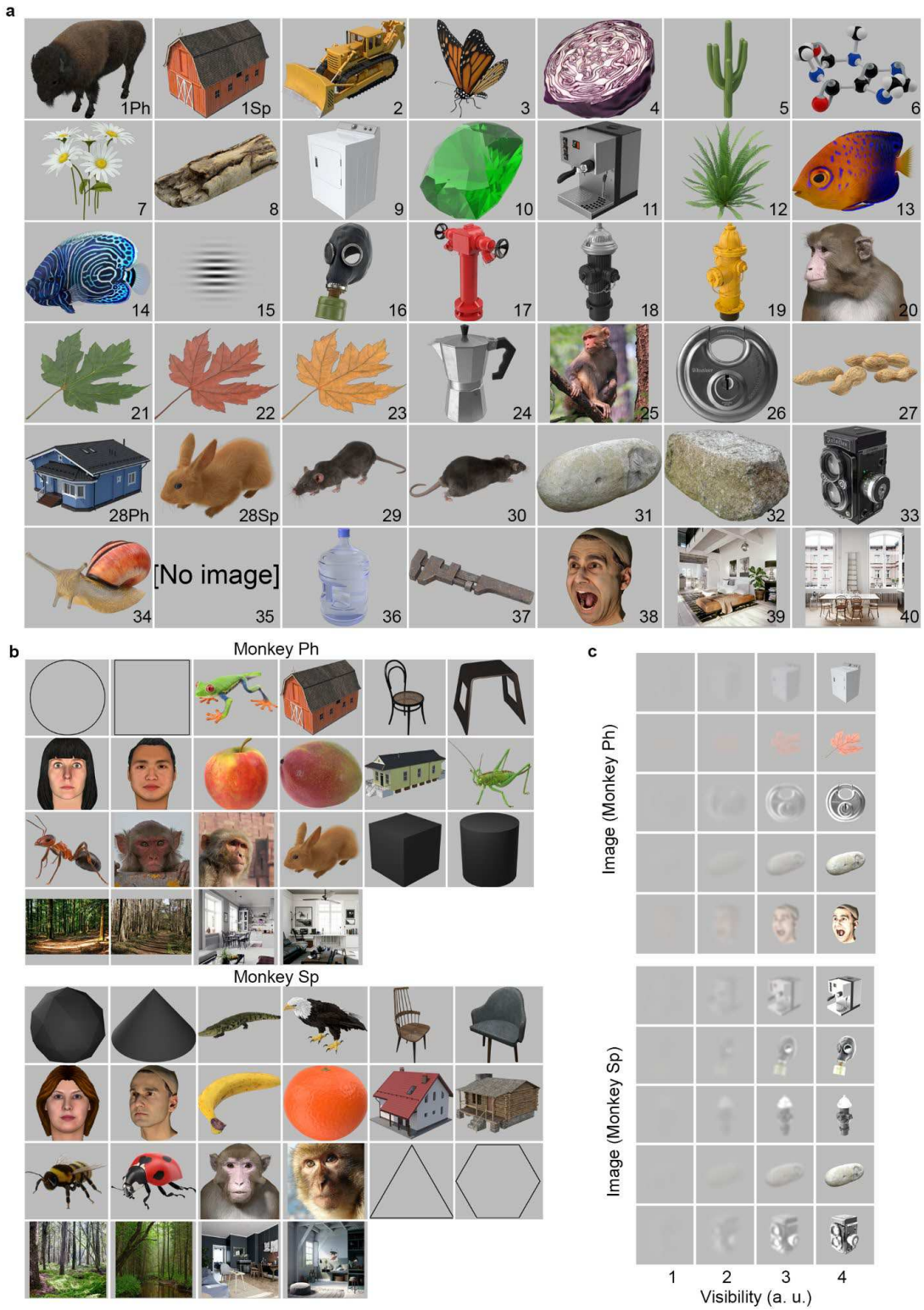

Figure S1. Visual stimuli. **a)** the images used in Experiment 1 and 2 for both monkeys. The images appeared as object cut-outs on a gray background as shown here. The images were

constrained within an imaginary 8°x8° central square except for Image 39 and 40 which were displayed at 30°x30°. Image 1Ph and 28Ph were only shown to monkey Ph, image 1Sp and 28Sp were only shown to monkey Sp. “Image” 35 was the “no image” condition and the “no image” text did not appear in the experiment. **b)** Images used during the training phase for each monkey. The last row of images for each monkey were displayed at 30°x30°. **c)** Image stimulus used in Experiment 3 for each monkey. All images were displayed at 8°x8°.

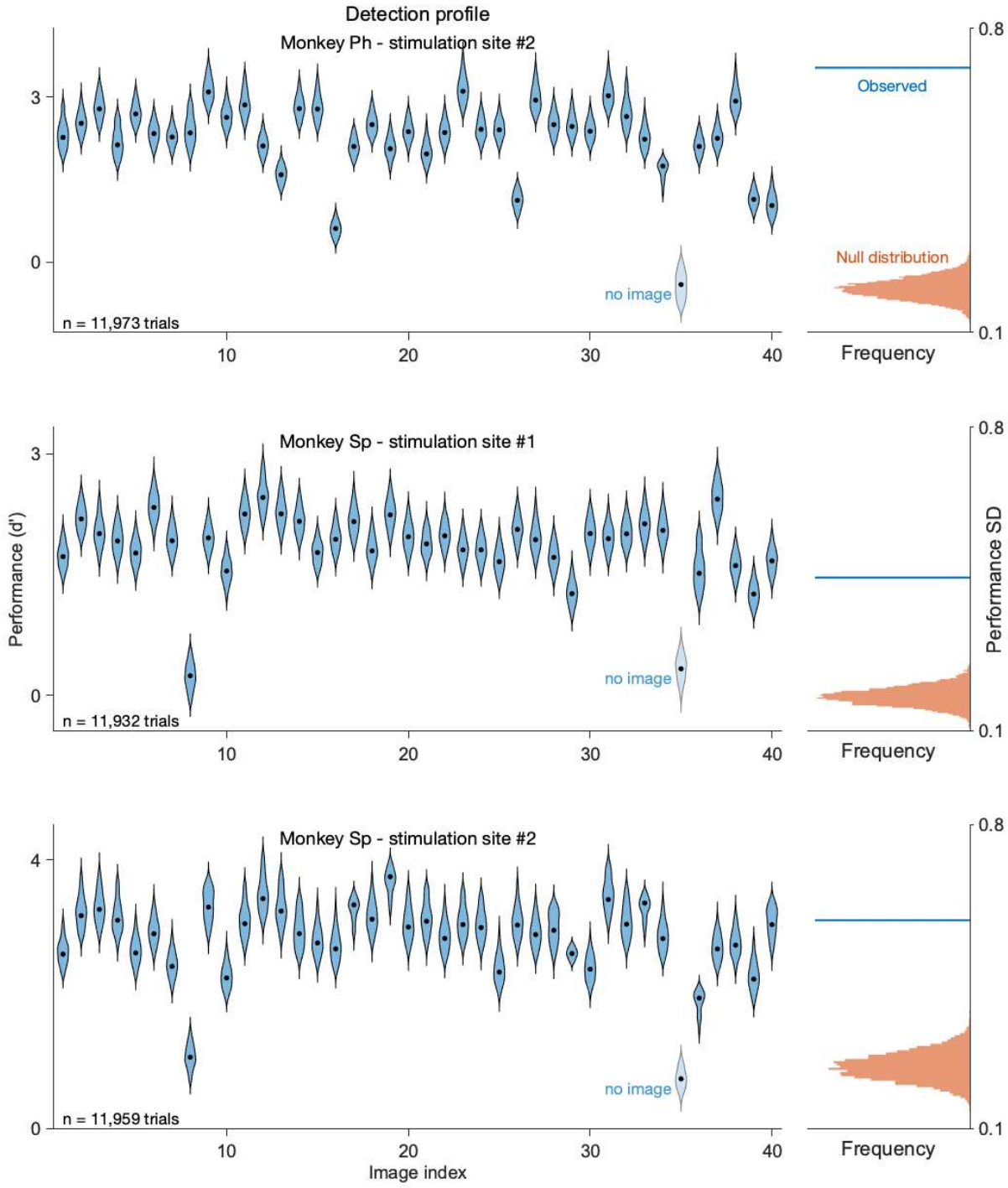

649

650 **Figure S2.** Detection profiles. See Figure 2.a

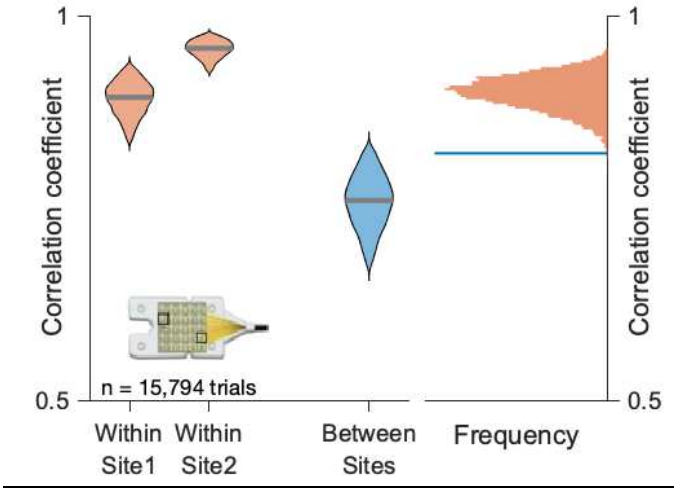

Figure S3. Correlation between detection profiles within and between stimulation sites. See Figure 2.b

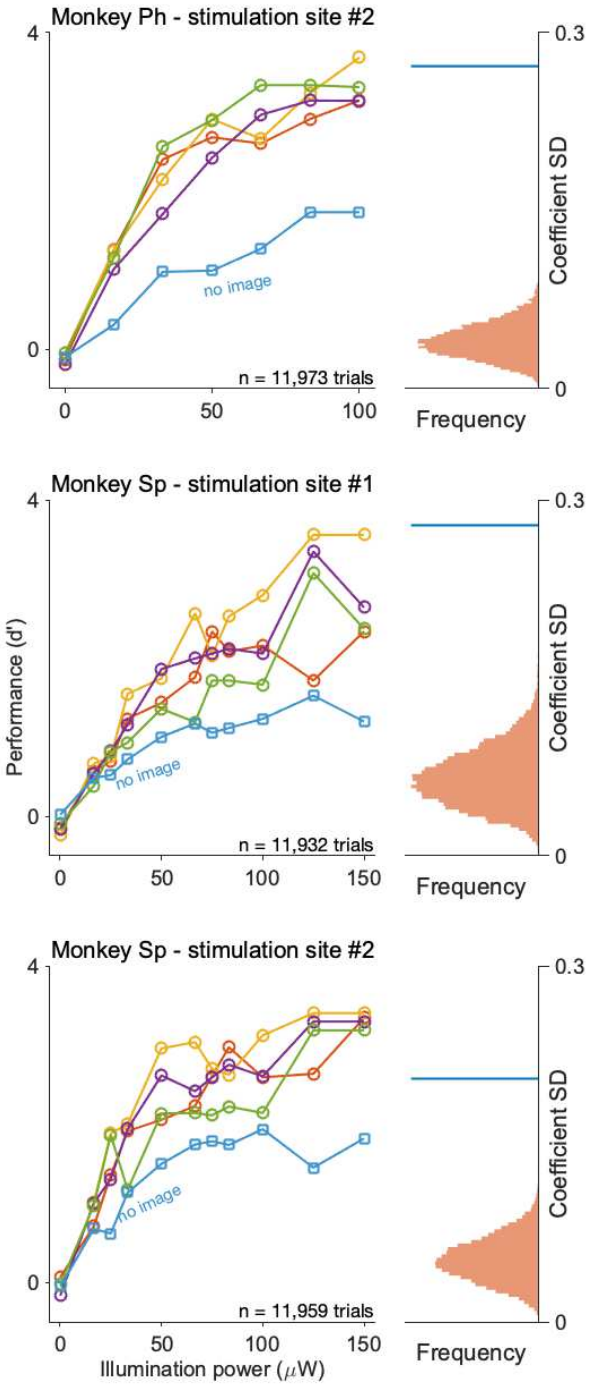

654

655 **Figure S4.** Psychometric functions. See Figure 2.c

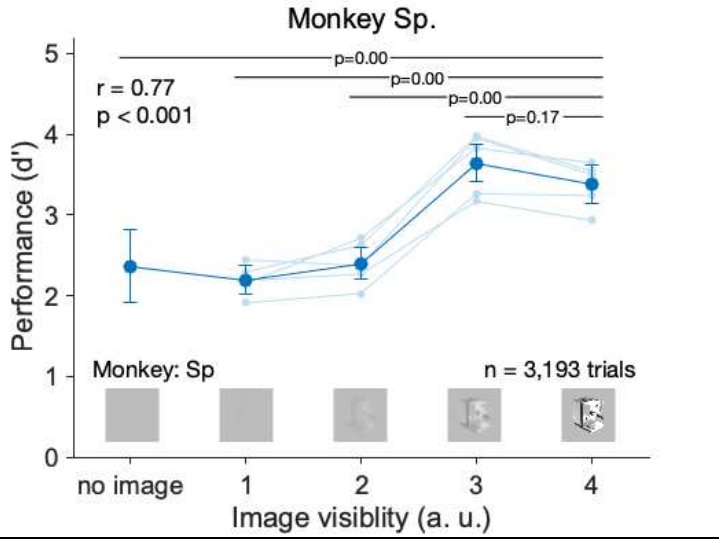

Figure S5. Stimulation detection performance is modulated by image visibility. See figure 3.b.